

Supporting Information

Dependence of Pharmacokinetics and Biodistribution on Polymer Architecture: Effect of Cyclic Versus Linear Polymers

Norased Nasongkla^{1,3}, Bo Chen¹, Nichole Macaraeg¹, Megan E. Fox², Jean M. J. Fréchet², Francis C. Szoka^{1*}

Departments of Biopharmaceutical Sciences and Pharmaceutical Chemistry, School of Pharmacy, University of California at San Francisco¹, 513 Parnassus Ave. HSE 1145, San Francisco, CA 94143-0912, Department of Chemistry, University of California, Berkeley², California 94720-1460, Department of Biomedical Engineering, Faculty of Engineering, Mahidol University³, Nakorn Pathom, Thailand

*To whom correspondence should be addressed: Email: szoka@cgl.ucsf.edu. Phone: (+1) 415-476-3895. Fax: (+1) 415-476-0688.

Materials. ϵ -Caprolactone (CL) was dried over CaH_2 , distilled under reduced pressure. α -Chloro- ϵ -caprolactone (CICL) and α -(1-acryloxyethyl)- ϵ -caprolactone (ACL) were synthesized as reported in literature.^{1, 2} 1,4-butanediol were azeotropically dried with toluene and distilled over a short-path apparatus in vacuo. 2,2-dibutyl-2-stanna-1,3-dioxepane (DSDOP) was synthesized following the procedure in literature.³ Toluene was refluxed over Na/K alloy /benzophenone and distilled under nitrogen. CH_2Cl_2 refluxed over P_4O_{10} . Gel Permeation Chromatography (GPC) was carried out by Viscotek (Houston, TX) VE 1122, RI detector (VE 3580) and right/low angle light scattering (270 Dual Detector) equipped with 2 size exclusion column (Polymer Laboratories) ResiPore, 300x7.5 mm, 3 μm particle size).

Synthesis of linear and cyclic poly(α -chloro- ϵ -caprolactone-co- ϵ -caprolactone).

The polymerization of ϵ -caprolactone (CL) and α -chloro- ϵ -caprolactone (CICL) were initiated in toluene by DSDOP following the procedure reported by Kricheldorf.³ ϵ -Caprolactone and α -chloro- ϵ -caprolactone were dried by azeotropic distillation of toluene. Then, toluene and initiator (DSDOP in toluene, 1 M) were successively added. The polymerization was allowed to occur for 2h at 40 °C. Then, ACL (cyclic) or CL (linear) was added to the polymerization medium ($[\text{ACL}]_0/[\text{DSDOP}]_0 = 15:1$). ACL, a crosslinker monomer, is subsequently polymerized into the random copolymer of the former two monomers to allow the cyclization via intramolecular photocrosslinking. Copolymerization medium was diluted with toluene ($[\text{Sn}] = 2.8 \times 10^{-4}$ M) and irradiated by UV (Medium pressure mercury-vapor lamp 450 W, 0.3-0.4 W/cm^2 , Ace Glass) at RT for 2.75 h in the presence of 1 mol% benzophenone with respect to the acrylic units. A sample was withdrawn after heating for 2h at 60 °C and hydrolyzed into the linear polymer precursor by a few drops of 1 M acetic acid in toluene. The polymer was precipitated in cold methanol and characterized by nuclear magnetic resonance (NMR) and gel permeation chromatography

(GPC) after UV photocrosslinking. ¹H NMR spectrum of the linear polymer precursor confirms the copolymer structure of ClCL and CL and the presence of acrylic units (chemical shift at 5.7-6.4 ppm). The copolymer ratio (ClCL:CL) of linear and cyclic polymer are the same at 42:58 (Table S1). After UV crosslinking, the intramolecular crosslinking was confirmed by the disappearance of three vinylic protons of α -(1-acryloxyethyl)- ϵ -caprolactone (chemical shift at 5.7-6.4 ppm) from the linear polymer precursor (Figure S1). GPC was used to confirm the formation of cyclic architecture from the linear polymer precursor.(Figure S2) Figure S3 (A-C) shows the plot between log MW and elution time which indicates more compact structure of cyclic polymer compared to linear polymer (linear polymer was eluted faster).

Table S1. Copolymer ratio and molecular weight of polymer

Polymer	Copolymer ratio (% mol)			Molecular weight		
	CL	Cl-CL	α A-CL	M _n	M _p	PDI
Linear polymer precursor	55	39.8	5.2	11407	13575	1.46
Cyclic polymer	58	42	0	9432	11353	1.38

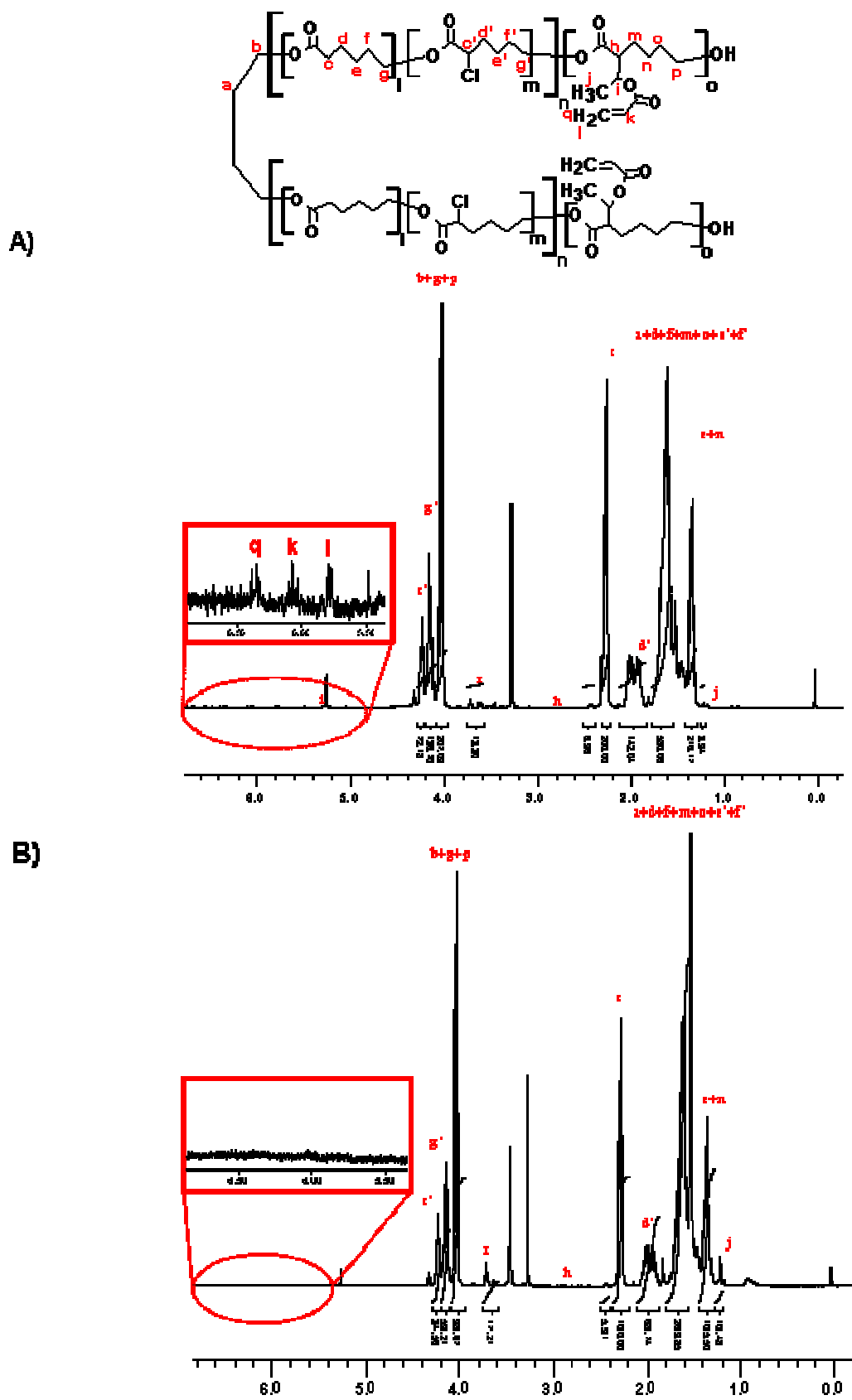


Figure S1. NMR (^1H , 400 MHz) of A) Linear B) Cyclic poly(α -chloro ϵ -caprolactone-co- ϵ -caprolactone)-block-(α -acryloxy- ϵ -caprolactone).

Figure S3B-C also shows that the cyclic structure of polymers is conserved after PEG grafting on the PCL backbone. Mark-Houwink plots (Figure S4) shows that the cyclic polymers have lower intrinsic viscosity than that of linear polymers at the same molecular weight. The $R_{h,cyclic}/R_{h,linear}$ ratio of PCL backbone is 0.86 which is consistent to the literature value ($R_{h,cyclic}/R_{h,linear} = 0.86-0.90$).⁴ The SEC system used to characterize the polymers consisted of a Waters 717plus Autosampler, Waters 515 HPLC pump, and 3 PLgel (7.5 x 300 mm, 5 mm particle size) columns in series, with pore size of 105, 103, and 500 Ang, respectively, a Wyatt Tech Dawn EOS (MALS), a Wyatt Tech Optilab DSP Interferometric Refractometer (RI), and a Wyatt Tech Viscostar (viscometer), in that order. THF was used as the eluent, run at 1.0 mL/min. The columns were held at 35 °C. Data was analyzed using the program ASTRA v.5.3.2.13. ASTRA will calculate the Mark-Houwink plots and the log(MW) vs elution time plots. The THF SEC system is calibrated with polystyrene standards. The average the "dn/dc" for each polymer was determined by changing the polymer concentrations for the calculation of the MW and viscosity of each sample.

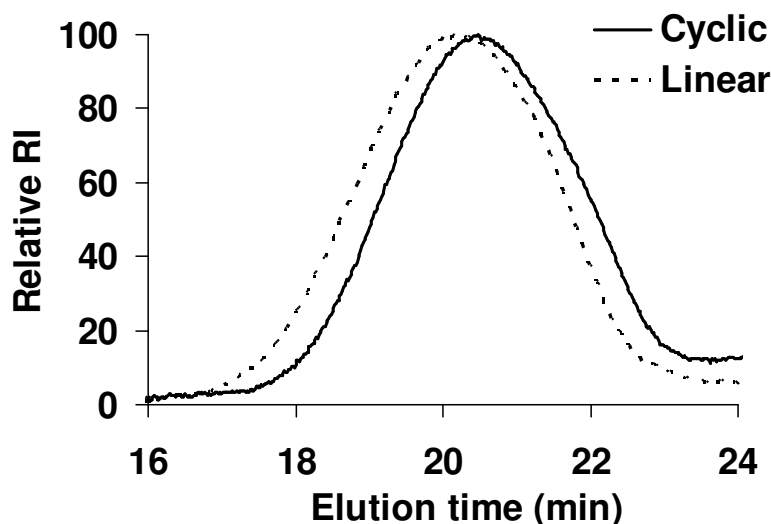


Figure S2. Gel permeation chromatography (GPC) of cyclic and linear poly(α -chloro ϵ -caprolactone-co- ϵ -caprolactone)

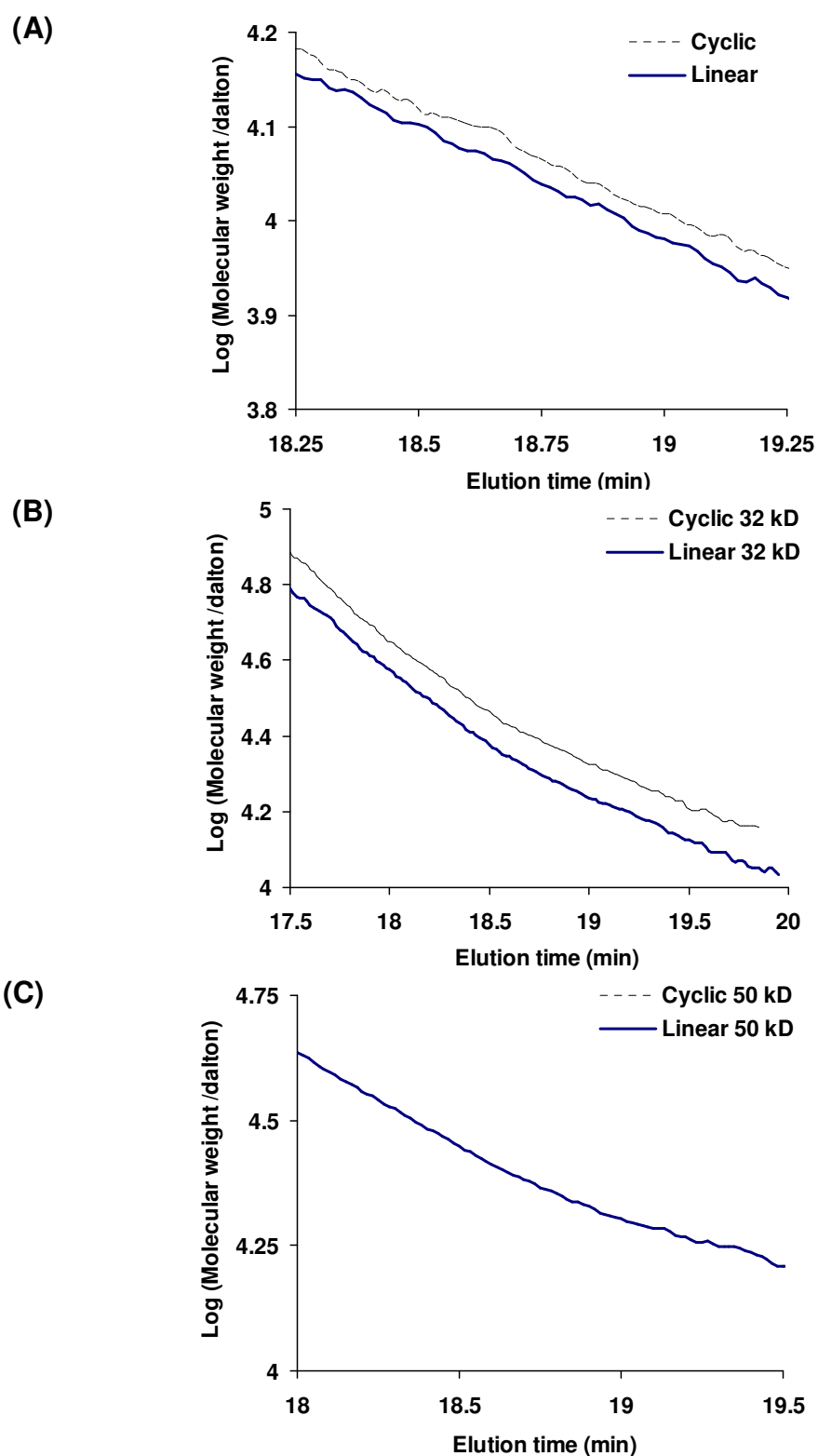


Figure S3. SEC plot between log molecular weight and elution volume of cyclic and linear polymers. (A) Cyclic and linear poly(α -chloro ϵ -caprolactone-co- ϵ -caprolactone)-block-(α -acryloxy- ϵ -caprolactone) (PCL 9 kD), (B) PEG(1.1 kD)-g-PCL (9 kD) and (C) PEG(2 kD)-g-PCL (9 kD).

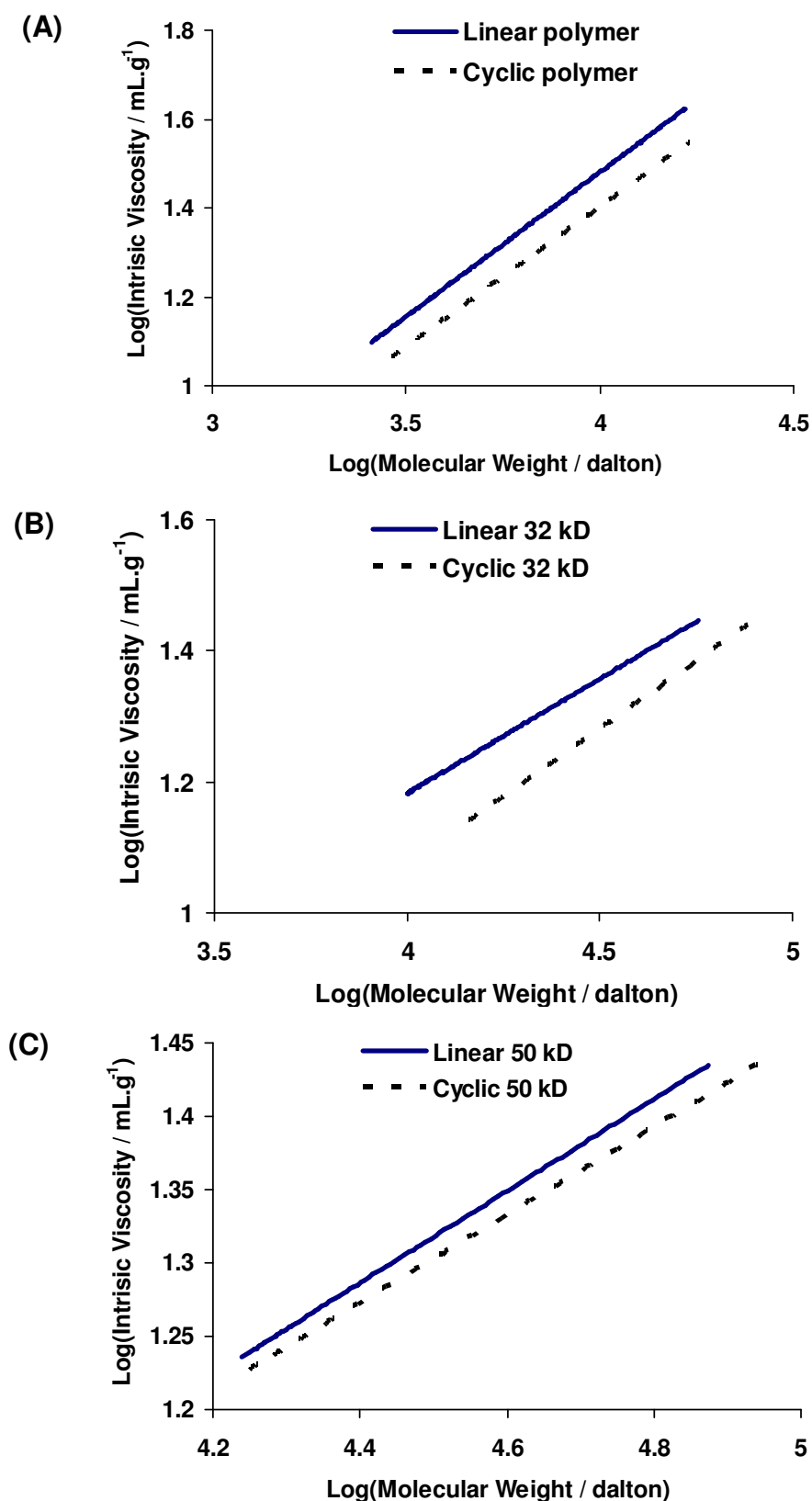


Figure S4. Mark-Houwink plots between log intrinsic viscosity and log molecular weight of cyclic and linear polymers. (A) Cyclic and linear poly(α -chloro ϵ -caprolactone-co- ϵ -caprolactone)-block-(α -acryloxy- ϵ -caprolactone) (PCL 9 kD), (B) PEG(1.1 kD)-g-PCL (9 kD) and (C) PEG(2 kD)-g-PCL (9 kD).

Synthesis of azide containing polymer (Poly(N₃CL-co-CL)). 0.2 gram of poly(α -Cl- ϵ -CL-co- ϵ -CL) (0.00135 mol of pendant chloride), and sodium azide 0.44 g (MW = 65.01) (0.00675 mol). The mixture was allowed to react in 5 mL DMF overnight at room temperature. The polymer was precipitated in cold methanol and characterized by nuclear magnetic resonance (NMR) and gel permeation chromatography (GPC).

Synthesis of propargyloxyphenol. Excess anhydrous K₂CO₃ (7.50 g) was added into a solution of the benzenediol (1.0 g, 9.08 mmol) in dry acetone (25 mL). The mixture was refluxed for 0.5 h then propargyl bromide (1.01g, 9.08 mmol) was added dropwise over a period of 5 h through a syringe pump. The resulting mixture was refluxed overnight and then cooled, filtered and the filtrate was evaporated. The brown oily residue was dissolved in CH₂Cl₂ (25 mL) and the solution was washed with water (2 x 10 mL) followed by saturated brine solution (10 mL). The organic layer was dried over anhydrous Na₂SO₄ then solvent was removed. The crude product was purified by column chromatography on silica gel eluted with hexane/ethyl acetate (19:1 v/v). The product was obtained with 47% yield. Figure S5 shows that NMR spectrum of propargyloxyphenol.

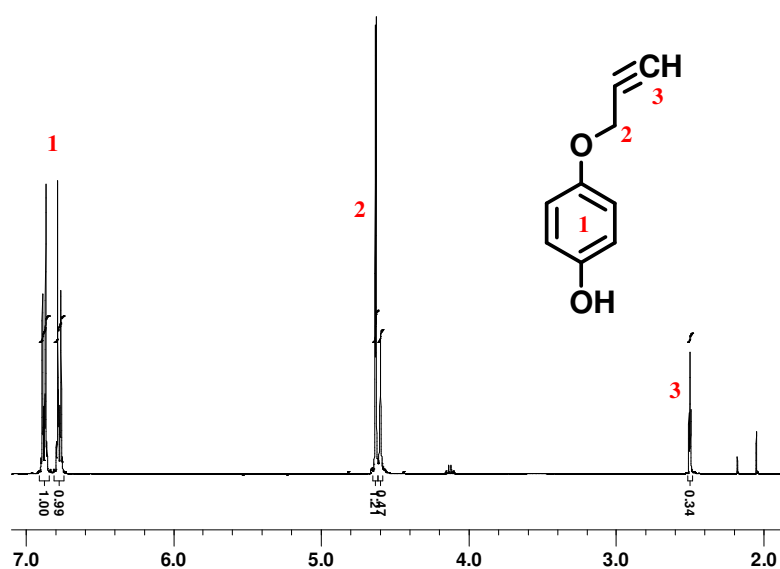
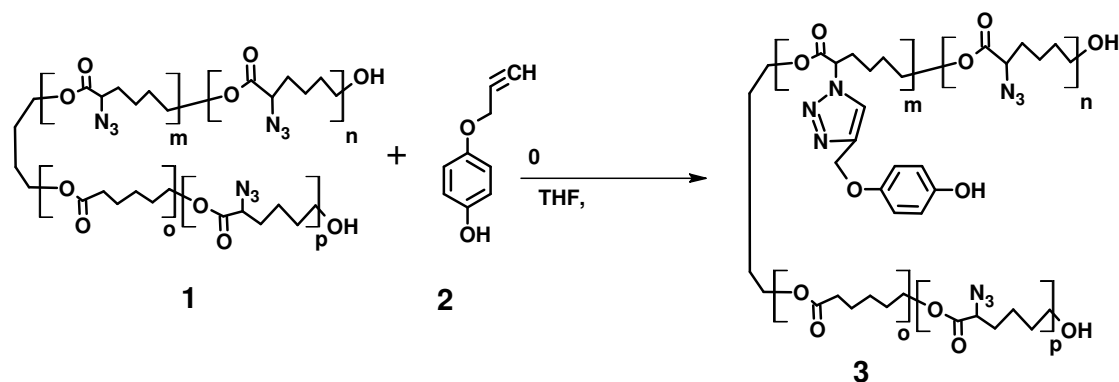


Figure S5. NMR (¹H, 400 MHz) of propargyloxyphenol.

Introduction of phenol moiety on polymer by click chemistry (Phenol-g-PCL) (**scheme S1**). 0.1 gram of poly(N₃CL-co-CL) **1** (0.232 mmol of pendant N₃,) and 0.00442 g CuI (0.1 eq, MW = 190.45) was dissolved in 3 mL THF. Propargyloxyphenol **2** (1.2 eq, 0.00028 mol, 0.0413 g) in 3 mL was added to rapidly stirring mixture. 3.23 μL of TEA (0.1 eq, MW=101.19) in 3 mL THF was added and purged with argon for 5 min before adding. The reaction was carried out at 40 °C for 2h. Polymer **3** was precipitated in cold methanol and characterized by NMR.



Scheme S1. Introduction of phenol moiety on polymer by click chemistry.

Synthesis of propargyl containing poly(ethylene glycol). NaH (60% w/w in mineral oil, 27.2 mg (from 45.3 mg), 1.134 mmol, 1.1 equiv.) was added to a solution of poly(ethylene glycol) (PEG) with MW 1.1, 2 or 5 kD (1 g, 0.5 mmol) in 10 mL of THF at 0 °C with frequent venting. After stirring for 15 min, propargyl bromide (80% in toluene, 0.168 mL, 1.134 mmol, 1.1 equiv) was added slowly by syringe pump, and the mixture was stirred at 0 °C for 2 h and then 23 °C overnight. The reaction mixture was filtered and precipitated in cold ether. The product was characterized by NMR. Figure S6 shows NMR of propargyl containing poly(ethylene glycol). NMR shows the disappearance of hydroxyl proton of PEG (2.7 ppm) and appearance of propargyl proton at 2.4 ppm in stead. Integral intensity of chemical shift at 2.4 and methylene proton of PEG (3.6 ppm) confirmed the monofunctional PEG.

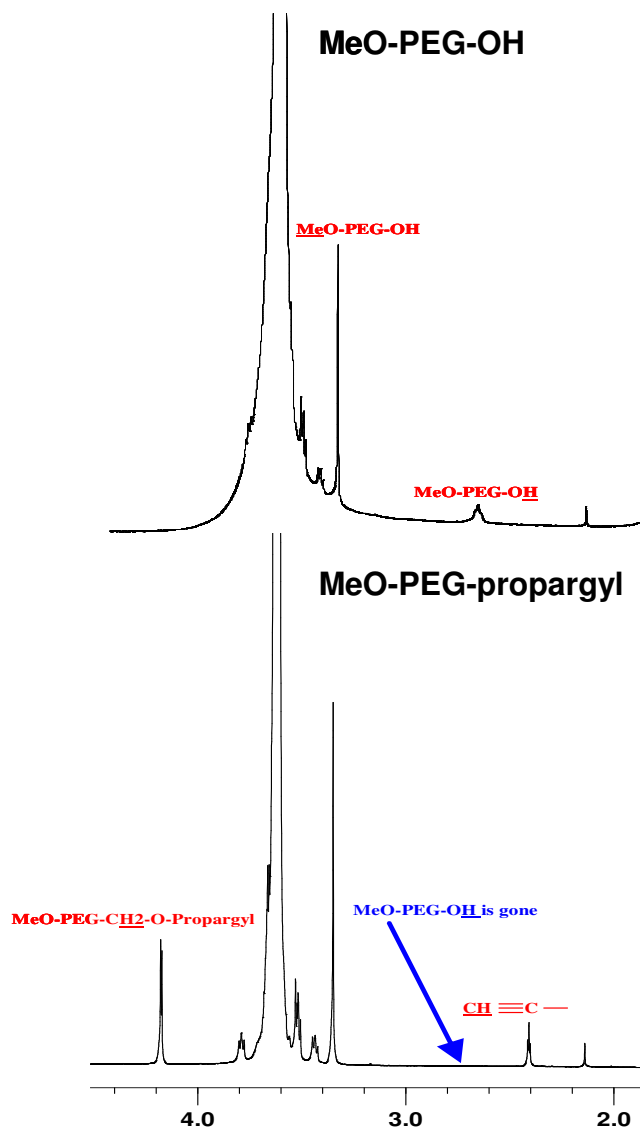


Figure S6. NMR (^1H , 400 MHz) of propargyl poly(ethylene glycol).

Introduction of PEG on polymer backbone by click chemistry. The polyester backbone was further modified by cycloaddition of α -alkyne, ω -methoxyl-PEG. PEG was grafted on P($\text{N}_3\text{CL-co-CL}$) at low temperature (40 $^\circ\text{C}$), low copper (0.1 equiv) and non aqueous condition (tetrahydrofuran) to avoid the hydrolytic degradation as reported by Lecomte et al. who recently showed the route to graft PEG on Poly(ClCL-co-CL) without degradation.⁵ More over, Emrick et al. reported that these polyester-g-PEG are biocompatible.⁶ 0.18 gram of poly($\text{N}_3\text{CL-co-CL}$) **1** (0.493 mmol of pendant N_3) and PEG 1.2

eq were dissolved in 10 mL THF. 9.4 mg CuI (0.1 eq, MW = 190.45) was dissolved in 3 mL THF and added to the mixture. Next, 6.9 μ L of TEA (0.1 eq, MW=101.19) was added and the reaction was carried out at 40 °C overnight. Polymer **3** was precipitated in cold hexane and the nongrafted PEG chains were eliminated by dialysis against ethanol. Figure 1 shows the ^1H NMR spectrum and the assignment of the signals of phenol moiety and PEG grafted poly($\text{N}_3\text{CL-co-CL}$). NMR confirmed the grafting of PEG by a characteristic chemical shift of $-\text{CH}_2\text{O}-$ resonance at 3.6 ppm and the triazole proton is observed at 7.7 ppm. The number of grafted PEG chains on the linear and cyclic polyester backbone was the same and calculated from the integral intensity of the chemical shift at 3.6 ppm ($-\text{CH}_2\text{O}-$) and 4 ppm ($-\text{CH}_2\text{CH}_2\text{CH}_2\text{O}-$). On average, 21 PEG chains were grafted onto poly($\text{N}_3\text{CL-co-CL}$) (72 units) so the number average molecular weight of grafted polymers were 32 and 50 kD for PEG 1.1 and 2 kD conjugation, respectively. The grafting efficiency of PEG 5 kD is relatively lower than that of PEG 1.1 and 2 kD. As a result, the number of grafted PEG chains was lower (15 grafted PEG chains) possibly due to steric hindrance and larger molecular size of PEG 5 kD chains. The number average molecular weight of grafted polymer was 90 kD. In contrast, a smaller molecular size of propargyl phenol compound **2** led to a uniform grafting efficiency. The chemical shift at 6.7 ppm (dd) is a characteristic peak of the benzene-1,4-diol protons. The integral intensity of this peak and PCL proton (4 ppm) were used to calculate the number of phenol moiety on polyester chain. On average, it is found that one polyester chain contains one phenol moiety. Figure S7 shows NMR spectra of PEG (1.1 kD) grafted linear polymer in D_2O and CDCl_3 , respectively. It is found that the polyester backbone (4.1, 2.2 to 0.8 ppm) solvates in both D_2O and CDCl_3 suggesting that it is not a core-shell structure.

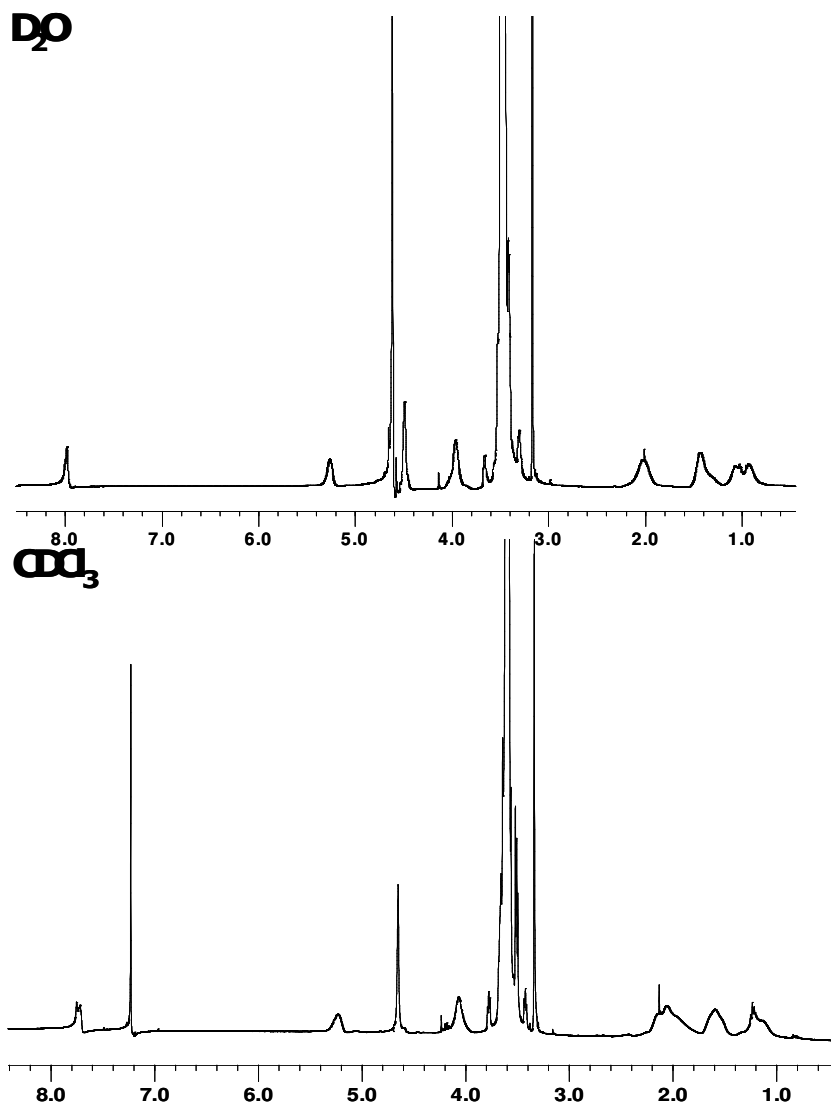


Figure S7. Attachment of propargyl poly(ethylene glycol) 1.1 kD on poly(α -chloro ϵ -caprolactone-co- ϵ -caprolactone) linear polymer.

The successful conjugation of PEG (2 kD) to polyester backbone is also confirmed by GPC (Figure S8). A significant shift toward higher MW was observed for both linear (13.2 to 12.8 mL) and cyclic (13.5 to 12.9 mL) polymer.

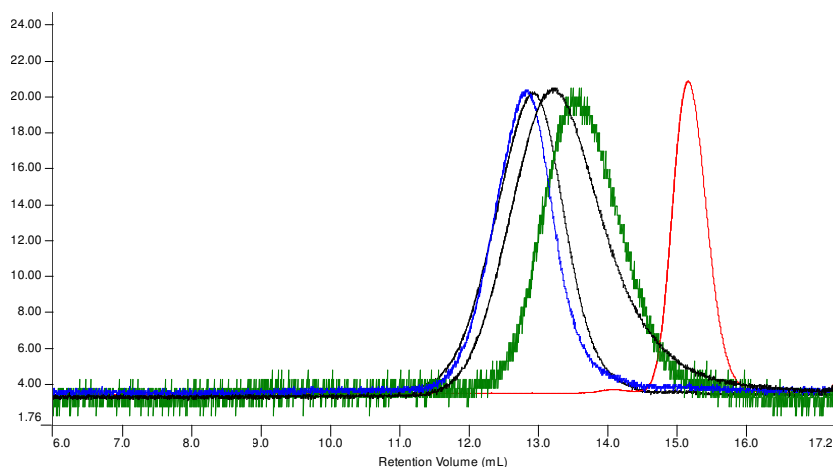


Figure S8. Gel permeation chromatography of Phenol-PEG-g-linear polymer, Phenol-PEG-g-cyclic polymer, linear P(CICL-co-CL), cyclic P(CICL-co-CL) and PEG 2 kD (from left to right).

***In vitro* degradation study of polymer in phosphate buffer saline (PBS) pH 7.4 and plasma.** Ten mg of polymer was dissolved in 10 mL of PBS. Polymer solutions were incubated at 37 °C and samples (1 mL) were withdrawn at the specific time over a period of 10 days. Samples were kept at -80 °C until they were ready to remove salt by running solutions through PD-10 desalting columns (GE Healthcare) in distilled water. Then polymers were lyophilized. For the plasma degradation study, a stock solution of polymers in PBS was made at 20 mg/mL. For each time point, approximately 0.8 mg of polymers was added to 160 μ L preheated human plasma (Sigma) and mixed by vortex mixer. Samples were then incubated at 37 °C. At specific time points, a mixture of 100 μ L water, 100 μ L methanol and 4.08 mg ZnSO₄ was added into polymer solutions to precipitate proteins. Samples were vortexed, centrifuged at 14,000 rpm for 5 min then frozen at -80 °C until they were ready for GPC.

Figure S9 shows *in vitro* degradation of linear (A) and cyclic (B) polymer in PBS, pH 7.4 at 37 °C. There was no significant degradation of polymers within 1 day. Linear and cyclic polymer showed the same degradation rate (Figure S9). A slight increase in polydispersity was observed after 1 day. A lower molecular weight, PEG 1.1 kD peak at 16.2 mL was detected. However, the major portion of materials was still observed at a higher

molecular weight up to 10 days. In comparison, a much higher degradation rate was detected in plasma. There was no significant degradation of polymers within 6 h.

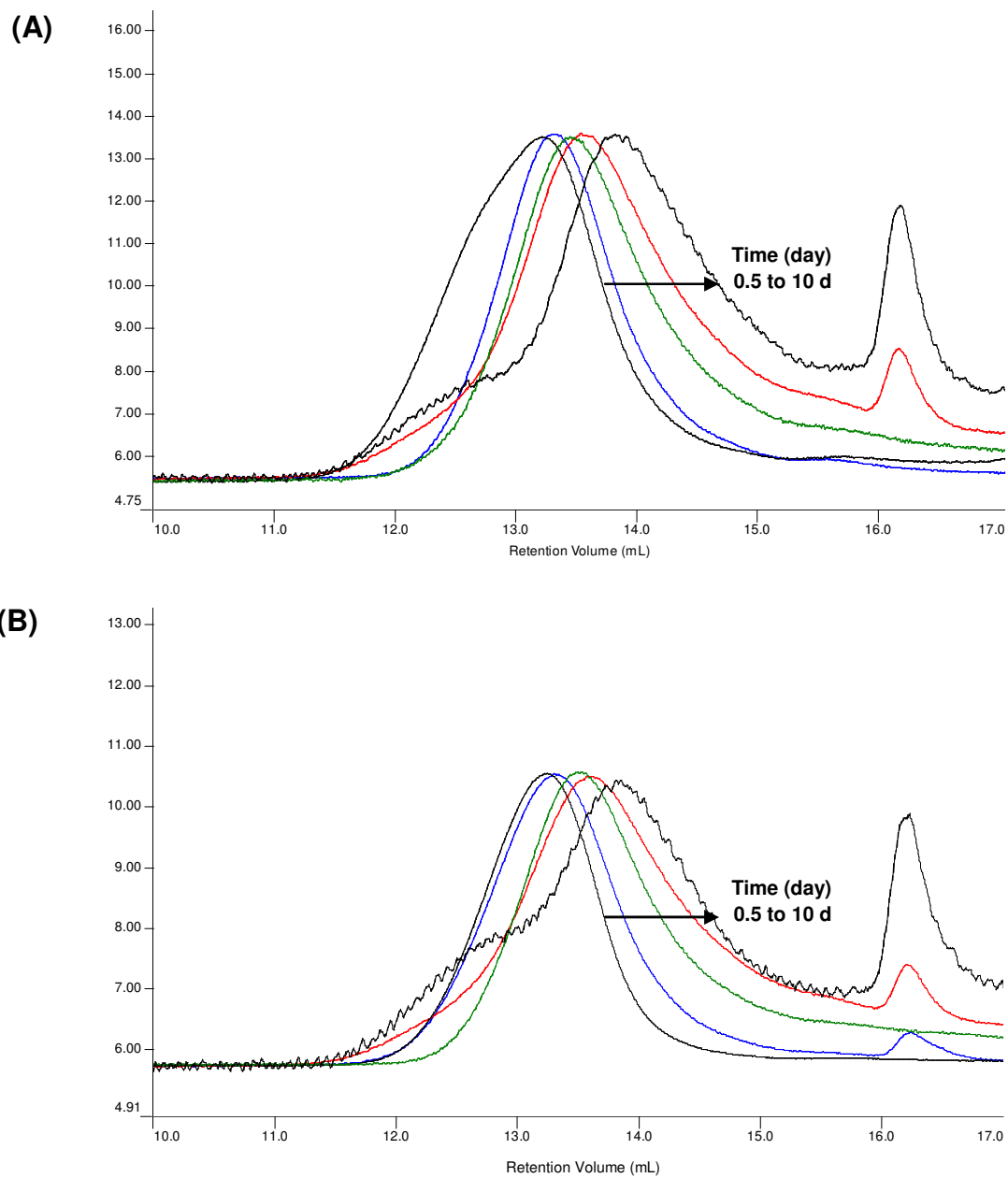


Figure S9. Time-dependent SEC profile of A) linear polymer and B) cyclic polymer incubated in PBS at 37 °C after 0.5, 1, 2, 4 and 10 days.

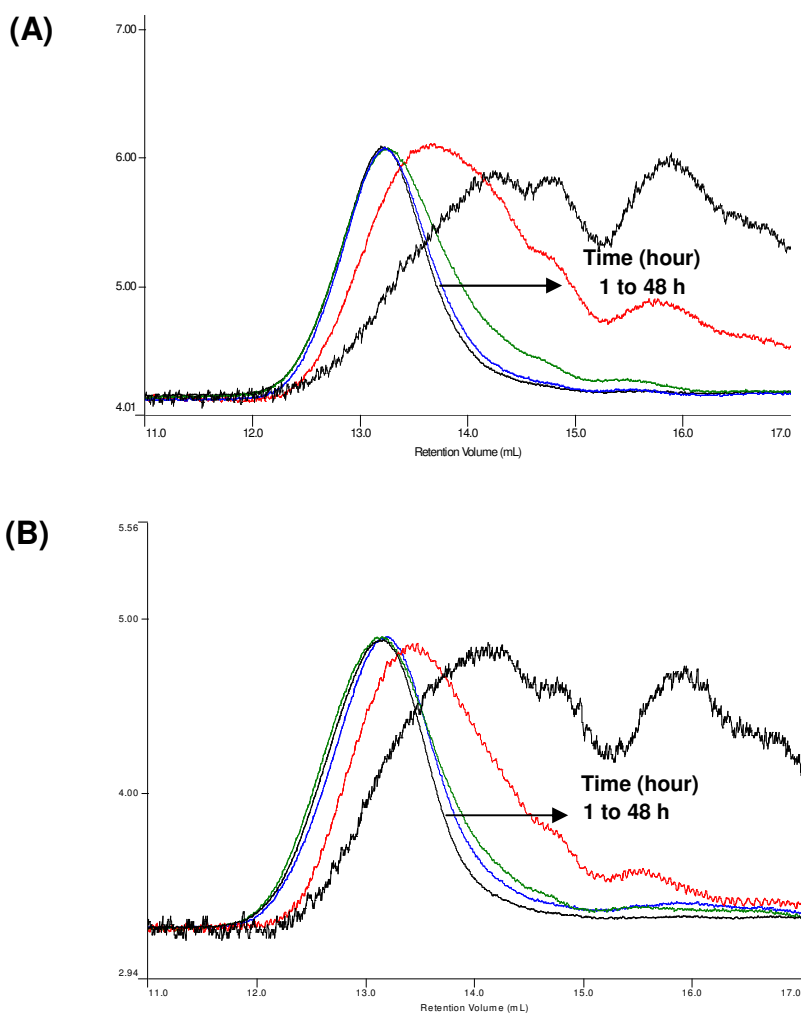


Figure S10. Time-dependent SEC profile of A) linear polymer and B) cyclic polymer incubated in human plasma at 37 °C after 1, 3, 6, 24 and 48 hour.

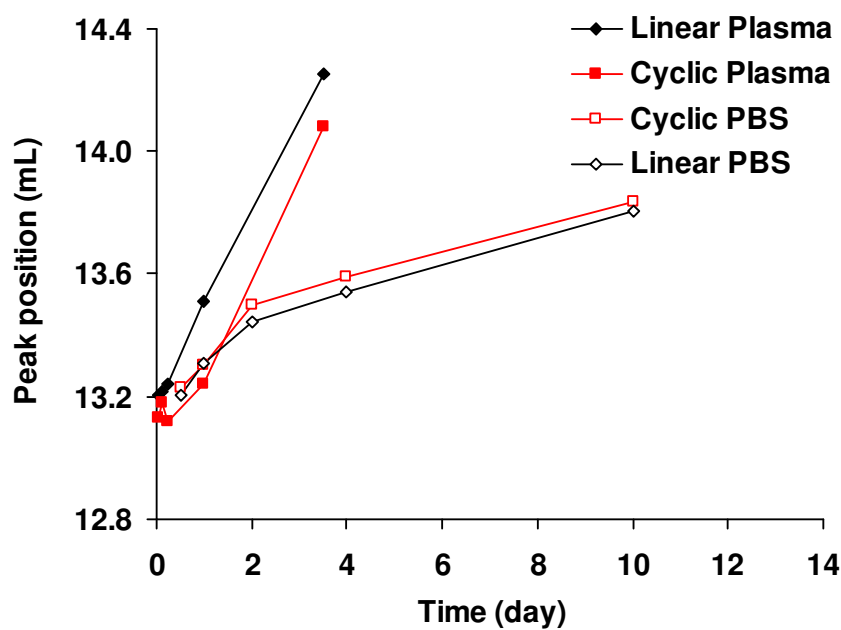


Figure S11. Plot of peak position (mL) against time as a result of degradation of polymer in plasma and PBS at 37 °C.

Radioiodination of phenol moieties of PEG grafted polymer. Phenol-functionalized polymers were iodinated as previously described.⁷ First, polymer (1 mg) were dissolved in 125 μL of borate buffer pH 8.5. A solution of potassium iodide (20 μL) and 10 μL of 14 mg/mL chloramines T solution were added into polymer solution. The reaction was carried out for 5 min then 40 μL of 38 mg/mL sodium metabisulfite was added to stop the reaction. The material was separated from iodide by placing the reaction mixture on an anion exchange column (Bio-Rad AG1-X2) in the chloride form and eluting it with 1.0 mL water. The polymer was further purified to remove any low MW radioactive contaminants from the polymer by SEC on Bio-Rad 10DG desalting columns that had been equilibrated with HBS (hepes buffer saline, 10 mM Hepes, 140 mM NaCl, pH 7.4). The high MW fractions eluted in 4 to 8 mL volume and were collected and pooled. A suitable quantity of radiolabeled polymer was mixed with cold polymer in sterile HBS to create a solution with 4 mg/mL polymer and specific activities of 4×10^6 CPM/mL.

Figure S11 shows the purification of linear and cyclic polymer with MW 50 kD by SEC on Bio-Rad 10DG desalting columns. The chromatogram of both linear and cyclic polymer confirmed the successful separation of polymer (4 to 8 mL) from low molecular weight contaminants (10 to 14 mL).

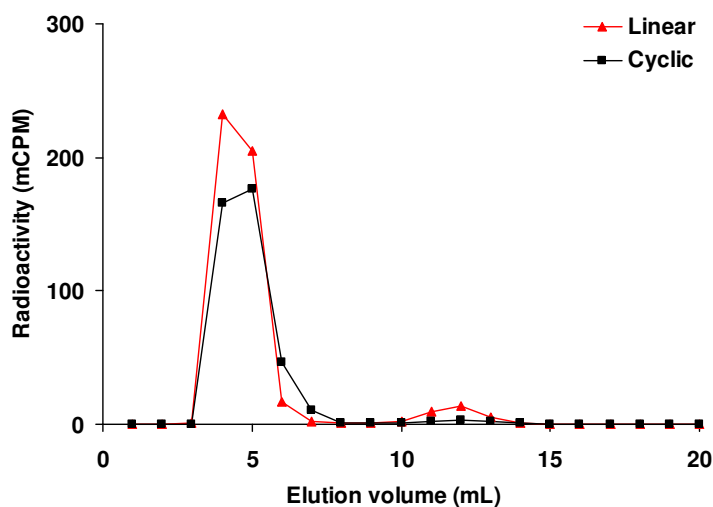


Figure S12. Purification of radiolabeled linear and cyclic polymer (50 kD) by size exclusion column.

To study the effect of iodination on polymer stability, polymers were subjected to iodination, as shown above, using non-radioactive potassium iodide (cold iodination). After purification by SEC, polymers were lyophilized and analyzed by GPC. Figure S13 shows the GPC of polymer subjected to cold iodination and the original polymer. It was found that iodination causes small shift of chromatogram and small increase of polydispersity.

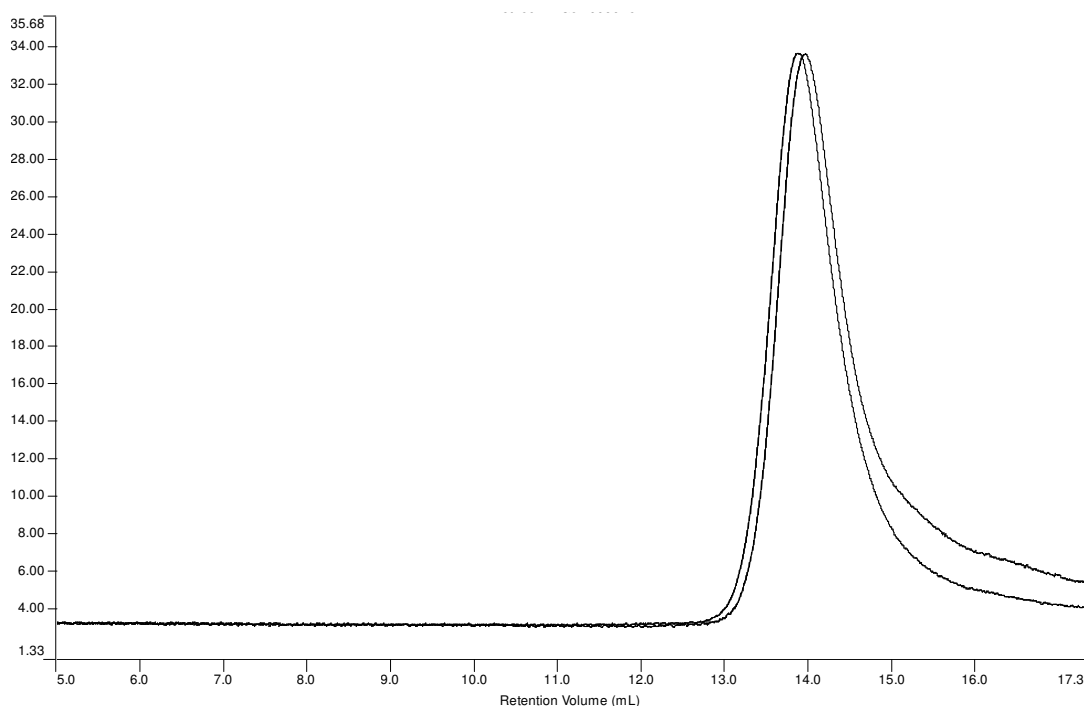


Figure S13. SEC of linear polymer (32 kD) before and after iodination.

Biodistribution Studies. Radioiodinated polymer solutions ($200 \mu\text{L}$, 1×10^6 CPM/mouse) were administered intravenously via the tail vein to 6-8-week old BALB/c female mice. The mice were sacrificed at two different time points (three mice per group) at 30 min and 24 h postinjection for biodistribution analyses. The blood (collected by heart puncture), heart, lungs, liver, stomach, spleen, GI, kidney, and carcass were collected, weighed and measured for radioactivity. Periodically, blood was also collected from the retroorbital sinus at intermediate time points to determine the dose of polymer in the blood. For the 24 h time points, mice were housed in metabolic cages to allow for the collection of urine and feces. The % injected dose per gram (% ID/g) of blood versus time curve was

analyzed using a two-compartment model (eq 1), since $\ln(\% \text{ ID/g})$ vs time curves clearly displayed two different elimination rates for the early and late time points. The pharmacokinetic parameters A , α , B , and β for the two compartment model were estimated using the residuals method. The elimination half-life was calculated as $(\ln 2)/\beta$, and the $\text{AUC}_{0 \rightarrow \infty}$ was calculated as $A/\alpha + B/\beta$. The concentration of polymer in the blood (C_p) at time t , is given by $C_p = A(e^{-\alpha t}) + B(e^{-\beta t})$

To determine if radioactivity in urine was polymer-associated or low MW-associated, the urine from mice treated with 50 kD linear and cyclic polymers were analyzed by chromatography on a G-50 Sephadex column ($1 \times 20 \text{ cm}$). Fractions were collected and analyzed for radioactivity as shown in Figure S14. It was found that the radioactivity from urine consisted of high (0 to 10 mL) to low (10 to 20 mL) MW associated materials where the low MW associated materials had the higher number of counts. Low MW materials arose due to the degradation of polymers which was observed in the degradation study (Figure S9, S10). The high MW associated materials peak may result from the partial degradation of polymers or the lower MW portion of intact polymers.

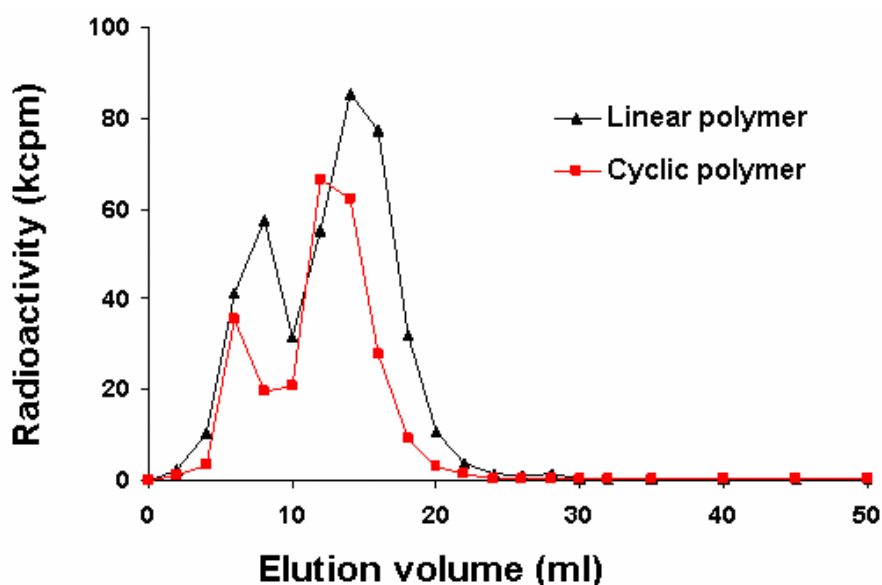


Figure S14. A plot of % recovered radioactivity from mice urine as a function of elution volume (mL).

To explore the cause of the rapidly eliminated fraction from blood of animals injected with the cyclic polymer, two mice were treated with cyclic polymer (10×10^6 CPM / mouse) then blood was withdrawn after 1 h. Then serum was separated and injected into a group of mice (0.4×10^6 CPM / mouse). Blood of the latter mice were collected and quantified for radioactivity. It was found that cyclic polymer isolated from serum had a higher concentration in blood at any time after injection and a longer blood circulation time compared to cyclic polymer with no pretreatment (Figure S15). The logarithmic plot shows a difference in the alpha phase, the cyclic polymer contained in the re-injected serum did not show as rapid a decrease in blood levels as observed with the un-manipulated cyclic polymer. The beta phases of the two polymers are similar. We suspect that the cyclic polymer that was in circulation after one hour was the high MW cyclic portion; any low molecular weight fragments in the initially injected material due to the iodination reaction (Figure S12) were eliminated in the first hour. In effect, the kidney was a biological filter to remove low molecular fragments

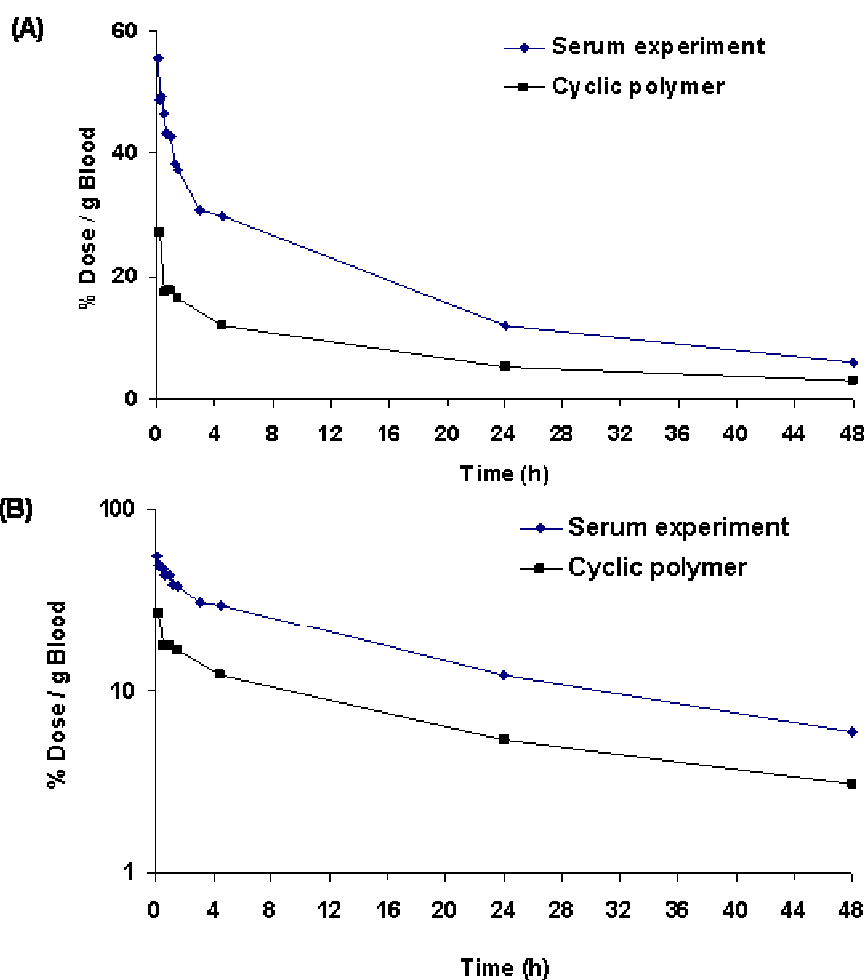


Figure S15. Plot of polymer concentration in the blood with respect to time. Figure B was plotted in log scale. Cyclic polymer refers to samples collected from the mice injected with the (50 kD) cyclic polymer. Serum experiment refers to samples from a second group of mice that had been injected with the serum collected one hour after the intravenous administration of the cyclic polymer in a first group of mice.

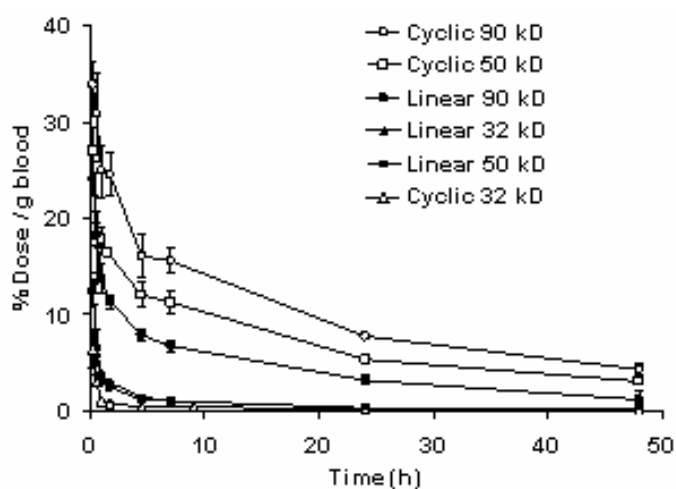


Figure S16. Plot of polymer concentration in the blood with respect to time.

References

1. Lenoir, S.; Riva, R.; Lou, X.; Detrembleur, C.; Jerome, R.; Lecomte, P., Ring-opening polymerization of alpha-chloro-is an element of-caprolactone and chemical modification of poly(alpha-chloro-is an element of-caprolactone) by atom transfer radical processes. *Macromolecules* **2004**, 37, (11), 4055-4061.
2. Li, H.; Debuigne, A.; Jerome, R.; Lecomte, P., Synthesis of macrocyclic poly(epsilon-caprolactone) by intramolecular cross-linking of unsaturated end groups of chains precyclic by the initiation. *Angew Chem Int Ed* **2006**, 45, (14), 2264-7.
3. Kricheldorf, H. R.; Eggerstedt, S., Macrocycles 2 - Living macrocyclic polymerization of epsilon-caprolactone with 2,2-dibutyl-2-stanna-1,3-dioxepane as initiator. *Macromolecular Chemistry and Physics* **1998**, 199, (2), 283-290.
4. Semlyen, J. A., *Cyclic Polymers*, 2nd ed.; Kluwer Academic Publishers: Dordrecht, The Netherlands, **2000**, Chapter 10, 347-384.
5. Riva, R.; Schmeits, S.; Stoffelbach, F.; Jerome, C.; Jerome, R.; Lecomte, P., Combination of ring-opening polymerization and "click" chemistry towards functionalization of aliphatic polyesters. *Chem Commun* **2005**, (42), 5334-6.
6. Parrish, B.; Breitenkamp, R. B.; Emrick, T., PEG- and peptide-grafted aliphatic polyesters by click chemistry. *J Am Chem Soc* **2005**, 127, (20), 7404-10.
7. Gillies, E. R.; Dy, E.; Frechet, J. M.; Szoka, F. C., Biological evaluation of polyester dendrimer: poly(ethylene oxide) "bow-tie" hybrids with tunable molecular weight and architecture. *Mol Pharm* **2005**, 2, (2), 129-38.